arXiv:nucl-ex/0512029v1 20 Dec 2005

Performance of ALICE silicon pixel detector prototypes in high energy beams

D. Elia[a,⋆], G. Anelli[b], F. Antinori[c], A. Badalà[d], G.E. Bruno[a], M. Burns[b], I.A. Cali[a,b], M. Campbell[b], M. Caselle[a], S. Ceresa[b], P. Chochula[b], M. Cinausero[e], J. Conrad[b], R. Dima[c], D. Fabris[c], R.A. Fini[a], E. Fioretto[e], S. Kapusta[b], A. Kluge[b], M. Krivda[f], V. Lenti[a], F. Librizzi[d], M. Lunardon[c], V. Manzari[a], M. Morel[b], S. Moretto[c], P. Nilsson[b], F. Osmic[b], G.S. Pappalardo[d], V. Paticchio[a], A. Pepato[c], G. Prete[e], A. Pulvirenti[d], P. Riedler[b], F. Riggi[d], L. Sándor[f], R. Santoro[a], F. Scarlassara[c], G. Segato[c], F. Soramel[g], G. Stefanini[b], C. Torcato de Matos[b], R. Turrisi[c], L. Vannucci[e], G. Viesti[c], T. Virgili[h]

[a] *Dipartimento IA di Fisica dell'Università and INFN, Bari, Italy*
[b] *CERN, Geneva, Switzerland*
[c] *Dipartimento di Fisica dell'Università and INFN, Padova, Italy*
[d] *Dipartimento di Fisica dell'Università and INFN, Catania, Italy*
[e] *Laboratori Nazionali di Legnaro, Legnaro, Italy*
[f] *Institute of Experimental Physics, Slovak Academy of Science, Košice, Slovakia*
[g] *Dipartimento di Fisica dell'Università and INFN, Udine, Italy*
[h] *Dipartimento di Fisica dell'Università and INFN, Salerno, Italy*

Abstract

The two innermost layers of the ALICE inner tracking system are instrumented with silicon pixel detectors. Single chip assembly prototypes of the ALICE pixels have been tested in high energy particle beams at the CERN SPS. Detection efficiency and spatial precision have been studied as a function of the threshold and the track incidence angle. The experimental method, data analysis and main results are presented.

Key words: Spatial precision, Efficieny, Silicon pixel detector, ALICE, LHC
PACS: 29.40.Gx, 29.40.Wk

⋆ Corresponding author, *E-mail address: Domenico.Elia@ba.infn.it*
on behalf of the SPD project in the ALICE Collaboration

1 Introduction

The ALICE experiment is dedicated to the study of the properties of QCD matter created in nucleus-nucleus collisions at LHC energies [1]. The inner tracking system in the ALICE apparatus is made of position sensitive detectors which have to handle several thousands tracks per unit of rapidity. The two innermost layers at 3.9 cm and 7.6 cm radii, respectively, constitute the Silicon Pixel Detector (SPD). The spatial precision and hit efficiency of the SPD are key parameters since they determine the ALICE capability of detecting particles with open heavy-flavour [2].
The basic detector unit of the ALICE SPD is the ladder, a two-dimensional silicon matrix of p^+n reverse biased diodes of dimensions 50 x 425 μm^2, flip-chip bonded to five read-out chips. Each diode is connected to a cell of the front-end read-out ASIC via a Pb-Sn solder bump of 25 μm diameter. The detector contains nearly 10^7 active cells in total. The read-out is binary. To reduce the material budget, the sensor thickness is limited to 200 μm and the read-out chip wafers are thinned down to 150 μm. Further details can be found in [3].
Early prototypes of the ALICE SPD elements, in the form of single-chip assemblies, were tested in high energy proton/pion beams at the CERN SPS in 2002 and 2003. These assemblies were made with sensors of 200 μm and 300 μm thicknesses, while the read-out chips (unthinned) were 725 μm thick. Those beam tests were primarily aimed at evaluating the performance of the bump-bonded assemblies and of the read-out electronics. Spatial precision and hit efficiency studies would have in principle required a more precise tracking telescope. However we found that the performance of the tracking doublets, together with a detailed cluster analysis of the hits, can yield a good determination of the intrinsic spatial precision and detection efficiency of the pixel plane under test. In the following sections the main focus is on the results of the 2002 beam test, where the sensor thickness (200 μm) was the same as the one used in ladder production; a study of the detector performance as a function of the threshold and the track incidence angle is presented. Some comparisons with the main results for the thicker sensor are also discussed.

2 Experimental setup and data analysis

The 2002 test was carried out in the H4 beam line at the SPS with a 350 GeV/c proton beam [4]. The experimental setup is schematically shown in Fig.1. The assembly under test was placed between two assembly pairs (minibus doublets) that were used as tracking telescope. The assemblies were all positioned with the short (50 μm) pixel cell side aligned along the y axis. The transverse position and the tilt angle of the test plane with respect to the beam line could

be changed remotely using a stepping motor gearbox. The trigger signal was generated by a telescope of four scintillating counters.
Data was collected with different inclination angles of the test plane with respect to the beam line, corresponding to rotations along an axis parallel to the 425 μm cell size direction (x coordinate). An angle scan (from 0 to 30, in steps of 5 degrees) was performed for three different values of the threshold, around the typical operating setting (namely 185, 200 and 210 DAC units). [2]
A complete scan of the global detector threshold was performed only for the configuration with normal incidence angle tracks.
In 2003 another test was done in the same experimental area, with a 120 GeV/c proton/pion beam as well as with higher multiplicity secondaries from 158 A GeV/c indium ions hitting a lead target in front of the detector setup. In this case the detector under study was an assembly with a 300 μm thick sensor and the two tracking detectors in each minibus doublet had the short and the long pixel cell side, respectively, aligned to the y axis: this crossed geometry was adopted to optimize the measurement of the transverse position of the tracks in both x and y coordinates. For more details see [5,6].
The analysis method is mainly based on the following steps: the cluster analysis of the hits on the pixel planes, the alignment of the transverse position of the detectors, the beam track reconstruction by using the tracking doublets and the study of the residual distributions on the test plane: a detailed description can be found in [7,8]. Clusters on the test plane are assigned to the beam track when their distance from the track impact prediction is below a defined maximum (i.e a cut in the residual is applied). In Fig.2 the frequency of different cluster patterns, at 200 DAC threshold ($\approx$ 3,000 electrons) and for normal incidence tracks, is shown. Under these conditions most of the clusters are made by a single pixel (68%) or two pixels along the direction of the short cell side (27%), while patterns with more than two pixels along the 425 μm cell side are not found. The relative frequencies of the various cluster types, as shown in the following section, rapidly change with the threshold and the track incidence angle on the detector since they are mostly determined by charge sharing and geometrical effects.
In absence of charge sharing, all the charge carriers locally generated around the incident particle trajectory are collected on a single pixel cell. The spatial precision in this case is given by $L/\sqrt{12}$ (where L is the pitch size of the detection element), which for the ALICE SPD corresponds to:

$$\sigma^{ncs}_{pixel}(y) = 14.4\ \mu m \qquad \sigma^{ncs}_{pixel}(x) = 122.7\ \mu m \quad . \tag{1}$$

In order to obtain the intrinsic spatial precision of the detector, the tracking error has to be subtracted from the widths of the residual distributions. As

[2] The DAC value of 200 corresponds to about 3,000 electrons in the effective threshold. Each 15 units decrease in the DAC setting corresponds to about 1,000 electrons increase in the effective threshold, at least for DAC values above 150.

an approximation we have assumed the following expression:

$$\sigma^2_{pixel}(y) = \sigma^2_{resid}(y) - \sigma_{track}(y)^2 \tag{2}$$

where $\sigma_{resid}(y)$ is the sigma of the Gaussian fit to the measured y-residual distributions, while $\sigma_{track}(y)$ has been estimated to be about 6 μm [8].
The efficiency of the test plane is defined as the ratio between the number of events where a cluster correlated to the reconstructed track is detected, and the total number of reconstructed tracks. The efficiency calculation has been based on a large number of tracks and cross checked for uniformity across the whole detector surface.

3 Results

At normal track incidence and 200 DAC threshold mainly single pixel and double-y pixel clusters occur. The precision is determined by their relative abundance. In Fig.3(a) the total y-residual distributions (for all the cluster patterns) is shown. After subtracting the uncertainty on the telescope prediction, the global detector precision is found to be $\sigma_{pixel}(y) = (\ 11.1 \pm 0.2\ )\ \mu m$. Due to charge sharing effects, a particle crossing a pixel cell close to the edge may generate two-pixel clusters with improved precision in the impact localization. This explains the narrower double-y pixel cluster residual distribution shown in Fig.3(b). The spatial precisions corresponding to the two main cluster patterns separately are found to be:

$$\sigma^{cls1}_{pixel}(y) = (\ 11.5\ \pm\ 0.2\ )\ \mu m \qquad \sigma^{cls2}_{pixel}(y) = (\ 6.8\ \pm\ 0.3\ )\ \mu m \qquad . \tag{3}$$

The errors on these estimates have been calculated by taking into account both the contributions due to uncertainties in the widths of the residual distributions and uncertainty in the tracking precision. A similar study for the spatial precision along the long cell side coordinate is available only for the 300 μm sensor [7]. At a DAC setting of 200 the efficiency has been estimated to be above 99%. In the following sections the performance dependence on the detector threshold and the track incidence angle are discussed.

3.1 Detector performance as a function of the threshold

A complete threshold scan measurement was performed with tracks at normal incidence. A detailed study of the evolution of the detector response, in particular for the relative frequencies of the various cluster patterns, has been carried out and used to adjust the SPD simulation [8,9].
The dependence of the detector efficiency on the threshold is illustrated in

Fig.4, where results are compared with those for the 300 μm sensor assembly. The detectors are fully efficient in a wide plateau region (efficiency values above 99%). Due to the smaller amount of produced charge carriers, the values for the thin sensor detector are shifted towards lower thresholds, hence the plateau region itself is shorter.
The dependence of the spatial precision on the global threshold is shown in Fig.5, again compared with the corresponding result found for the 300 μm sensor. A steeper dependence on the threshold for the thin detector is found. The smooth lines are from a spline fitting algorithm. The absolute minimum in the precision for the 300 μm sensor is reached at the threshold for which single and double-y pixel clusters are equally frequent [7]. This condition for the thin sensor is not even reached at lowest threshold of 210 DAC ($\approx$ 2,000 electrons): this is shown in Fig.6 where the contributions of single and double-y pixel clusters to the intrinsic precision (a) and to the detection efficiency (b) are illustrated.
The thin detector precision curve reaches a maximum around 160 DAC setting, with a corresponding value closely approaching $L_y/\sqrt{12}$ (mostly single pixel clusters). Tracks impacting a cell close enough to the boundary region may share the produced charge almost equally in two adjacent pixels: for high thresholds (DAC values smaller than 160 for the 200 μm sensor case) it can happen that none of the two pixels are fired. For this reason below 160 DAC the sensitive region of the pixel cell is reduced: this explains the decrease of the intrinsic precision which appears at the same threshold setting where the efficiency also starts to decrease with respect to the plateau value.
The width of the charge sharing region increases for decreasing thresholds: this explains the increase of the precision curve for double pixel clusters when increasing the DAC setting. Below 190 DAC units ($\approx$ 4,000 electrons) mostly cluster patterns that would have been made by 3 or 4 pixels for softer thresholds enter the double-y pixel cluster sample, then making the corresponding average precision slightly worse. In addition, at high thresholds, the fraction of double pixel clusters created by charge sharing are expected to be negligible with respect those originated, for instance, from delta-rays.

3.2 Detector performance as a function of the track incidence angle

Data runs were taken with the detector under test tilted from 0 to 30 degrees and with thresholds set to 185, 200 and 210 DAC units. Fig.7 schematically shows pixel cells traversed by a track at three different incidence angles. As an example of the evolution of the cluster patterns by varying the track inclination angle, in Fig.8 we report the corresponding distributions for 10 (a) and 20 degrees (b), to be compared with that shown in Fig.2 for normal track incidence. For 10 degrees inclined tracks the two main cluster patterns are almost balanced, while at 20 degrees the double pixel clusters dominate.

Results of the study on the spatial precision as a function of the track incidence angles are shown in Fig.9. The precision curves reach the minimum around 5-10 degrees (equal fractions of single and double-y pixel clusters) then degrading for all the threshold settings with the increasing track angle. In Fig.9(b) the intrinsic precision is shown together with the contributions due to the main pixel cluster patterns separately, for the case of 200 DAC threshold setting. These results can be particularly useful in the tuning of the tracking errors to be associated to the SPD points, both in the simulation and in the data analysis.

4 Summary

The performance of prototype assemblies for the ALICE Silicon Pixel Detector have been extensively studied by using beam test data collected in the past years at the CERN SPS. The cluster pattern distribution, the intrinsic spatial precision and the detection efficiency have been investigated as a function of both the detector threshold and the incident angle of the tracks. The results show a very high detection efficiency (above 99%) in a wide threshold range and a spatial precision of about 10 μm in the short pixel side coordinate for normal track incidence and 210 DAC threshold. The detector performance with angled tracks has also been investigated.

References

[1] ALICE Collaboration, *Technical Proposal*, CERN/LHCC 95-71.

[2] ITS Technical Design Report, CERN/LHCC 99-12, 1999.

[3] P. Riedler *et al.*, these proceedings.

[4] P. Riedler *et al.*, Proceedings of the $PIXEL2002$ Workshop, Carmel (USA), published in the SLAC Electronics Conference archive.

[5] P. Nilsson *et al.*, Proceedings of the 10^{th} Vienna Conference on Instrumentation, Vienna (Austria), February 2004, NIM A 535 (2004) 424-427.

[6] A. Pulvirenti *et al.*, these proceedings.

[7] D. Elia *et al.*, ALICE Internal Note, ALICE-INT-2005-011.

[8] D. Elia *et al.*, ALICE Internal Note, ALICE-INT-2005-007.

[9] G.E. Bruno *et al.*, ALICE Internal Note, ALICE-INT-2005-022.

Figure caption

Fig. 1. Schematic view of the layout for the 2002 ALICE SPD beam test.

Fig. 2. Distribution of cluster patterns on the test plane, for tracks at normal incidence and threshold setting of 200 DAC units.

Fig. 3. Distributions of the y-residuals for all the pixel clusters (a) and for double-y pixel clusters only (b); σ_{resid} is the standard deviation of the Gaussian fit to each distribution.

Fig. 4. Detection efficiency as a function of the threshold for tracks at normal incidence, for both sensor thicknesses. The results of a fit with Gaussian-integral function are superimposed.

Fig. 5. Intrinsic spatial precision along the y coordinate for tracks at normal incidence, as a function of the threshold and for both sensor thicknesses.

Fig. 6. Contribution of single and double-y pixel clusters to the intrinsic precision (a) and to the detector efficiency (b) as a function of the threshold.

Fig. 7. Schematic picture of pixel planes crossed by tracks at different inclination angles in the yz planes. Pixel cells traversed by the track are shown in red.

Fig. 8. Cluster pattern distributions for threshold settings of 200 DAC units, for tracks at 10 (a) and 20 degrees (b) incidence angle.

Fig. 9. Intrinsic precision in the y coordinate as a function of the track incidence angle on the detector and at different threshold settings.

Fig. 10. Intrinsic y-precision as a function of the track incidence angle, at different thresholds (a) and at 200 DAC threshold for the main cluster patterns separately (b).

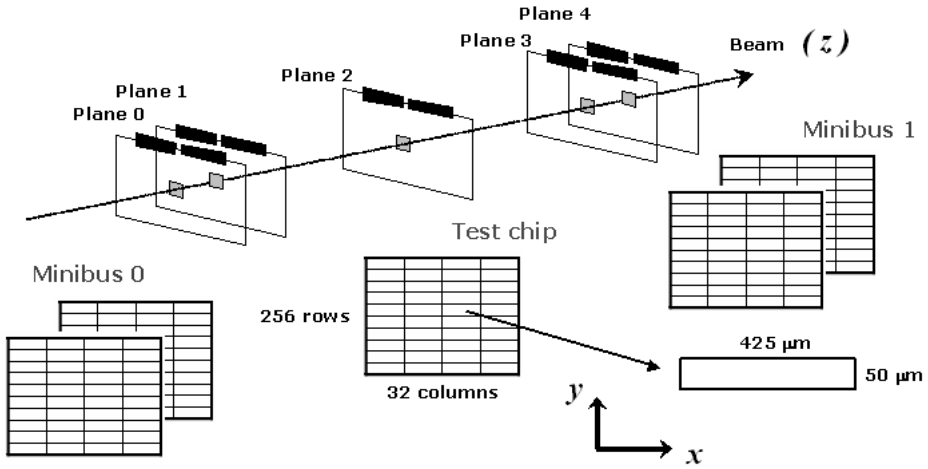

Fig. 1.

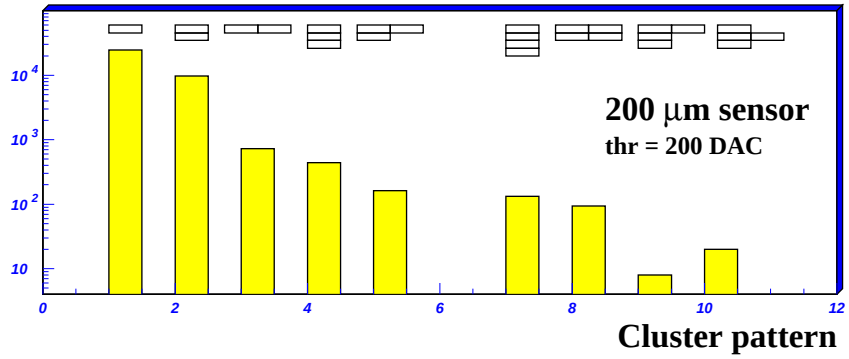

Fig. 2.

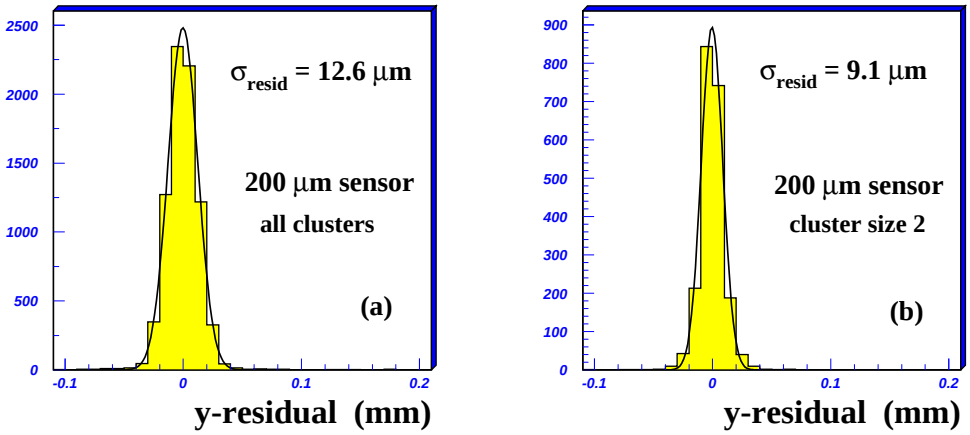

Fig. 3.

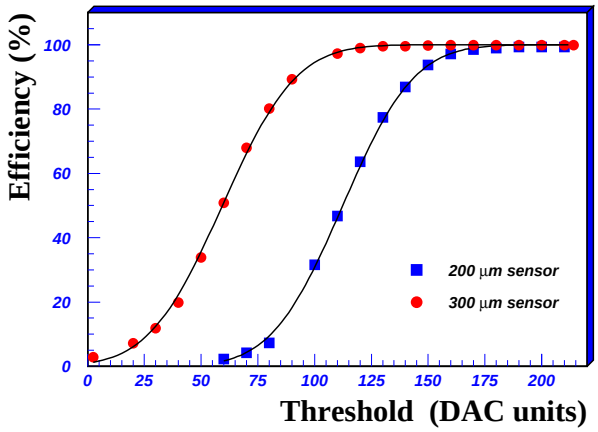

Fig. 4.

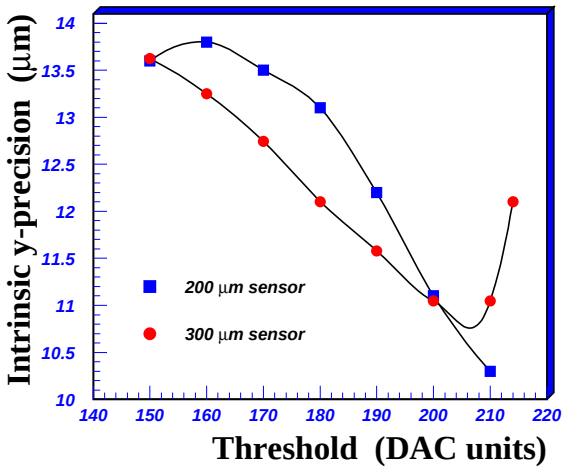

Fig. 5.

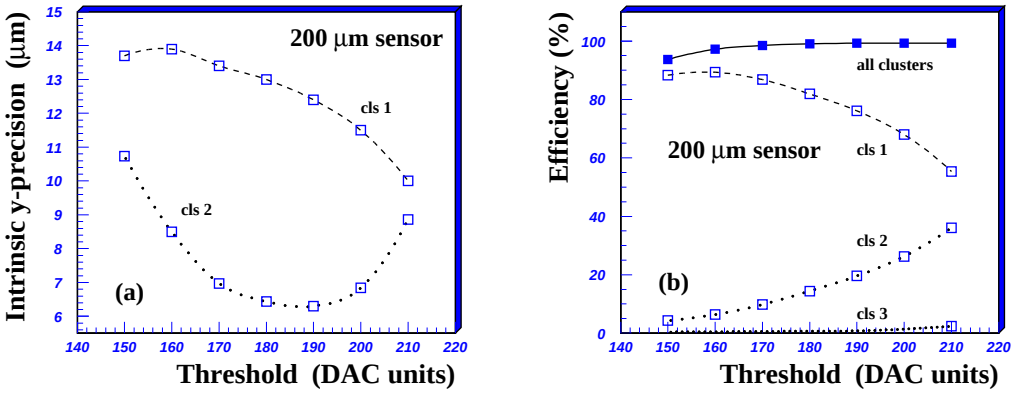

Fig. 6.

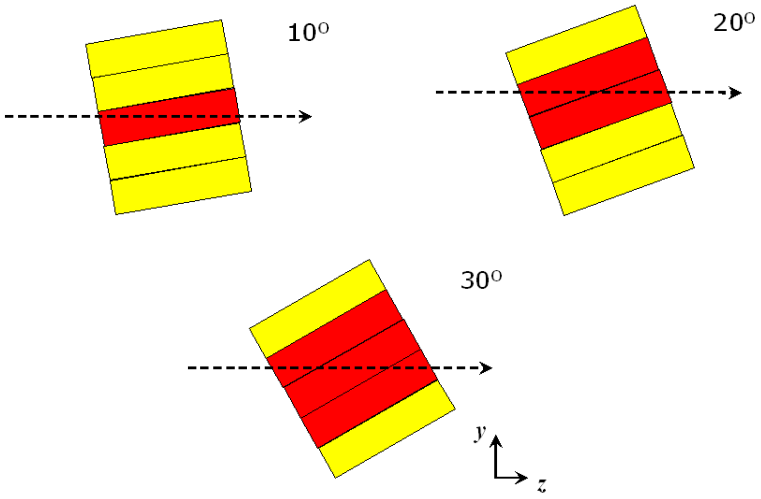

Fig. 7.

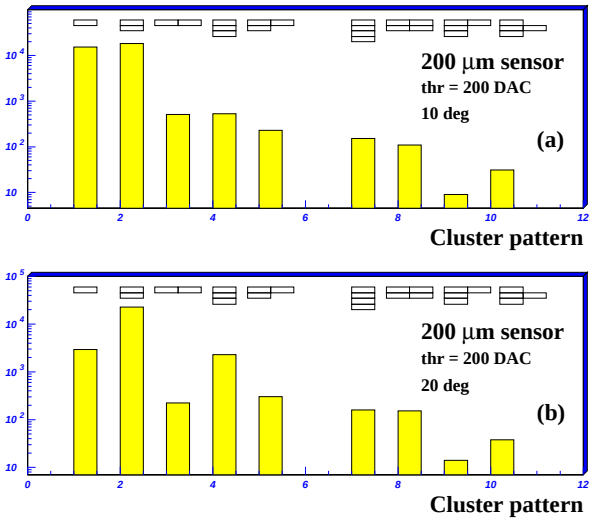

Fig. 8.

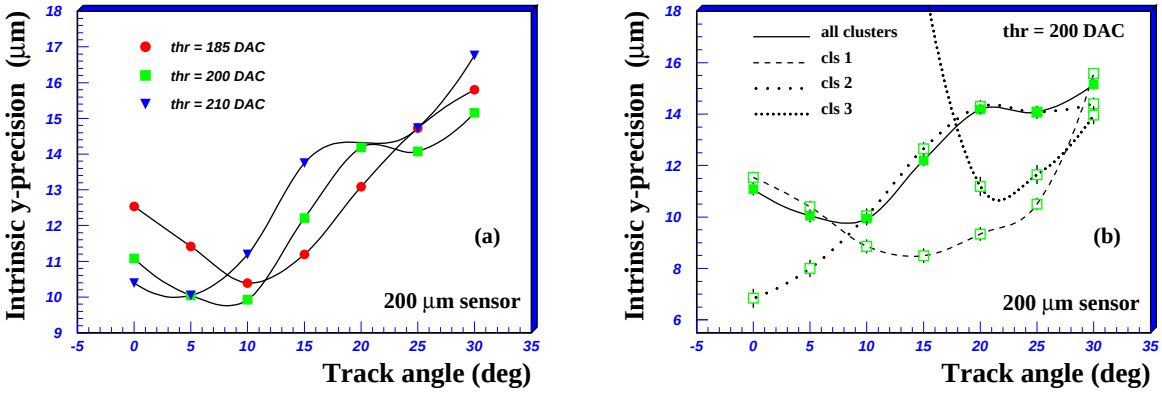

Fig. 9.